

## Supplementary Information

# Tracking spatiotemporal quantum interference in a double-well potential by femtosecond pulse-pair excitation: A theoretical study

Subho Mitra and Arijit K. De\*

*Condensed Phase Dynamics Group*, Department of Chemical Sciences, Indian Institute of Science Education and Research Mohali, Knowledge City, Sector 81, SAS Nagar, Punjab, 140306, India.

\*Corresponding author

Email: [akde@iisermohali.ac.in](mailto:akde@iisermohali.ac.in)

## Supplementary Information

### S1: Details of the computational methodology

The ground state wavefunction  $v''(r, 0)$  is launched into the first excited state upon time-delayed pulse-pair interaction and following the first-order perturbation theory, the time-dependent excited state wavepacket (WP) is written as,

$$v'(r, t) = \frac{i}{\hbar} \int_{-\infty}^t dt' \{ e^{-iH_e(t-t')/\hbar} [\mu_{eg} [E_1(t') + E_2(t')]] e^{-iH_g t'/\hbar} \} v''(r, 0) \quad (\text{S1})$$

Now, the time-dependent WP propagation in the excited state is numerically evaluated following the split-operator method using a grid-based spatial coordinate. If we consider the dimension of spatial and temporal grid to be  $m$  and  $n$  respectively, then from equation S1 the overall WP can be obtained as a spatiotemporal matrix *i.e.*, in the form of spatiotemporal quantum carpet (QC) and can be represented as follows,

$$v'(r, t) = \begin{bmatrix} v'_{11}(r_1, t_1) & v'_{12}(r_1, t_2) & v'_{13}(r_1, t_3) & \dots & v'_{1\tau}(r_1, t_\tau) & \dots & v'_{1n}(r_1, t_n) \\ v'_{21}(r_2, t_1) & v'_{22}(r_2, t_2) & v'_{23}(r_2, t_3) & \dots & v'_{2\tau}(r_2, t_\tau) & \dots & v'_{2n}(r_2, t_n) \\ v'_{31}(r_3, t_1) & v'_{32}(r_3, t_2) & v'_{33}(r_3, t_3) & \dots & v'_{3\tau}(r_3, t_\tau) & \dots & v'_{3n}(r_3, t_n) \\ \vdots & \vdots & \vdots & \vdots & \vdots & \vdots & \vdots \\ v'_{m1}(r_m, t_1) & v'_{m2}(r_m, t_2) & v'_{m3}(r_m, t_3) & \dots & v'_{m\tau}(r_m, t_\tau) & \dots & v'_{mn}(r_m, t_n) \end{bmatrix}_{m \times n} \quad (\text{S2})$$

where  $r_1, r_2, \dots, r_m$  denotes the spatial and  $t_1, t_2, \dots, t_n$  denotes the temporal grid. Each column in the matrix represents the corresponding WP at that particular time and each consecutive column is evaluated from the last time-evolved column. Therefore, the time-dependent WP after pulse-pair interaction at a time delay  $\tau$  is obtained as,

$$v'(r, t: t = \tau) = \begin{bmatrix} v'_{1\tau}(r_1, t_\tau) \\ v'_{2\tau}(r_2, t_\tau) \\ v'_{3\tau}(r_3, t_\tau) \\ \vdots \\ v'_{m\tau}(r_m, t_\tau) \end{bmatrix}_{m \times 1} \quad (\text{S3})$$

## Supplementary Information

Therefore, the complex conjugate of  $v'$  is,

$$v'^*(r, t: t = \tau) = [v'_{1\tau}{}^*(r_1, t_\tau) \quad v'_{2\tau}{}^*(r_2, t_\tau) \quad v'_{3\tau}{}^*(r_3, t_\tau) \quad \dots \quad v'_{m\tau}{}^*(r_m, t_\tau)]_{1 \times m} \quad (\text{S4})$$

As the space dependence is trivial, considering only the time-dependence, following the bra-ket notation, the outer product of  $v'$  and its complex conjugate is,

$$|v'(t)\rangle\langle v'(t)| = \begin{bmatrix} v'_{1\tau}(r_1, t_\tau) \\ v'_{2\tau}(r_2, t_\tau) \\ v'_{3\tau}(r_3, t_\tau) \\ \vdots \\ v'_{m\tau}(r_m, t_\tau) \end{bmatrix} \times [v'_{1\tau}{}^*(r_1, t_\tau) \quad v'_{2\tau}{}^*(r_2, t_\tau) \quad v'_{3\tau}{}^*(r_3, t_\tau) \quad \dots \quad v'_{m\tau}{}^*(r_m, t_\tau)]$$

$$= \begin{bmatrix} v'_{1\tau}(r_1, t_\tau)v'_{1\tau}{}^*(r_1, t_\tau) & v'_{1\tau}(r_1, t_\tau)v'_{2\tau}{}^*(r_2, t_\tau) & \dots & v'_{1\tau}(r_1, t_\tau)v'_{m\tau}{}^*(r_m, t_\tau) \\ v'_{2\tau}(r_2, t_\tau)v'_{1\tau}{}^*(r_1, t_\tau) & v'_{2\tau}(r_2, t_\tau)v'_{2\tau}{}^*(r_2, t_\tau) & \dots & v'_{2\tau}(r_2, t_\tau)v'_{m\tau}{}^*(r_m, t_\tau) \\ \vdots & \vdots & \vdots & \vdots \\ v'_{m\tau}(r_m, t_\tau)v'_{1\tau}{}^*(r_1, t_\tau) & v'_{m\tau}(r_m, t_\tau)v'_{2\tau}{}^*(r_2, t_\tau) & \dots & v'_{m\tau}(r_m, t_\tau)v'_{m\tau}{}^*(r_m, t_\tau) \end{bmatrix}_{m \times m} \quad (\text{S5})$$

Therefore, by summing over the diagonal elements of the equation S5, the excited state population as a function of interpulse delay  $\tau$  is obtained as,

$$P(\tau) = \text{Tr} (|v'(r, t: t = \tau)\rangle\langle v'(r, t: t = \tau)|)$$

$$= v'_{1\tau}(r_1, t_\tau)v'_{1\tau}{}^*(r_1, t_\tau) + v'_{2\tau}(r_2, t_\tau)v'_{2\tau}{}^*(r_2, t_\tau) + \dots + v'_{m\tau}(r_m, t_\tau)v'_{m\tau}{}^*(r_m, t_\tau)$$

$$= v'_{1\tau}{}^*(r_1, t_\tau)v'_{1\tau}(r_1, t_\tau) + v'_{2\tau}{}^*(r_2, t_\tau)v'_{2\tau}(r_2, t_\tau) + \dots + v'_{m\tau}{}^*(r_m, t_\tau)v'_{m\tau}(r_m, t_\tau)$$

$$= \langle v'(r, t: t = \tau)|v'(r, t: t = \tau)\rangle \quad (\text{S6})$$

## Supplementary Information

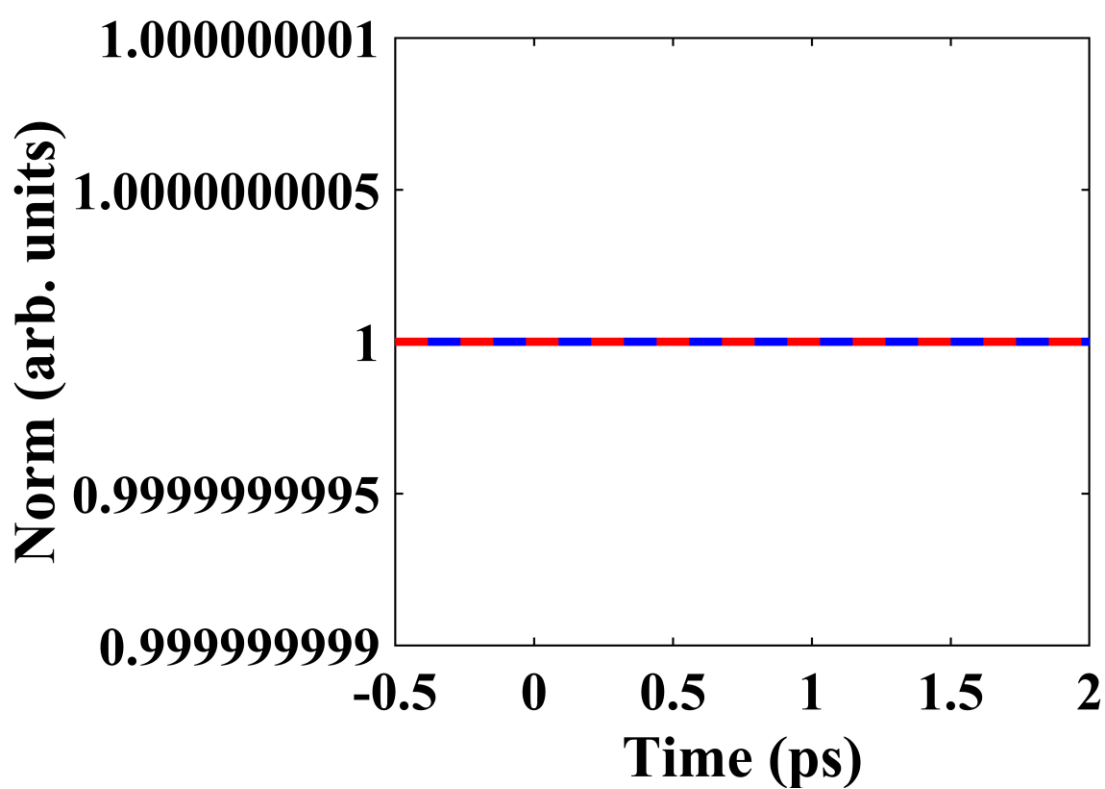


**Figure S1:** Norm of the excited state wavepacket upon pulsed excitation for two different sets of coordinate grid sizes. The plot shows that the norm remains invariant over time for the grid size of  $-10 \text{ \AA}$  to  $10 \text{ \AA}$  (shown in blue) and  $-20 \text{ \AA}$  to  $20 \text{ \AA}$  (shown in red) with 512 grid points.

## Supplementary Information

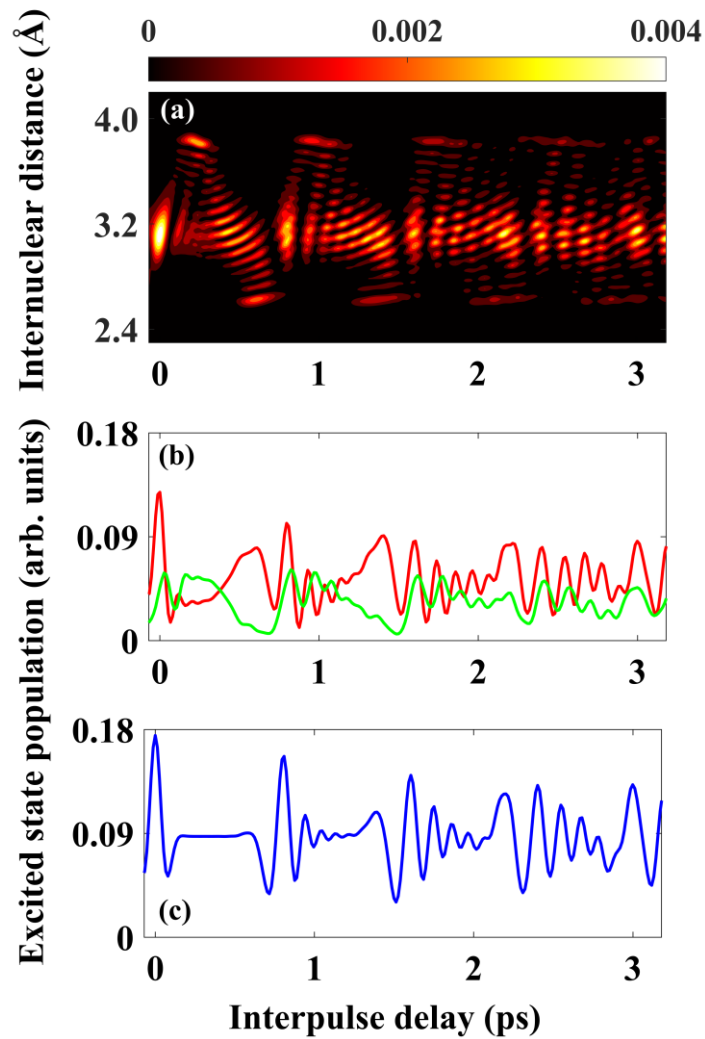


**Figure S2:** (a) Spatial mapping of excited state population as a function of interpulse delay after introducing a chirp of  $-1000 \text{ fs}^2$ . (b) Excited state population within the left well (shown in red) and the right well (shown in green) as a function of interpulse delay. (c) Total excited state population obtained by summing up both the contributions from the left and the right wells as a function of interpulse delay.

## Supplementary Information

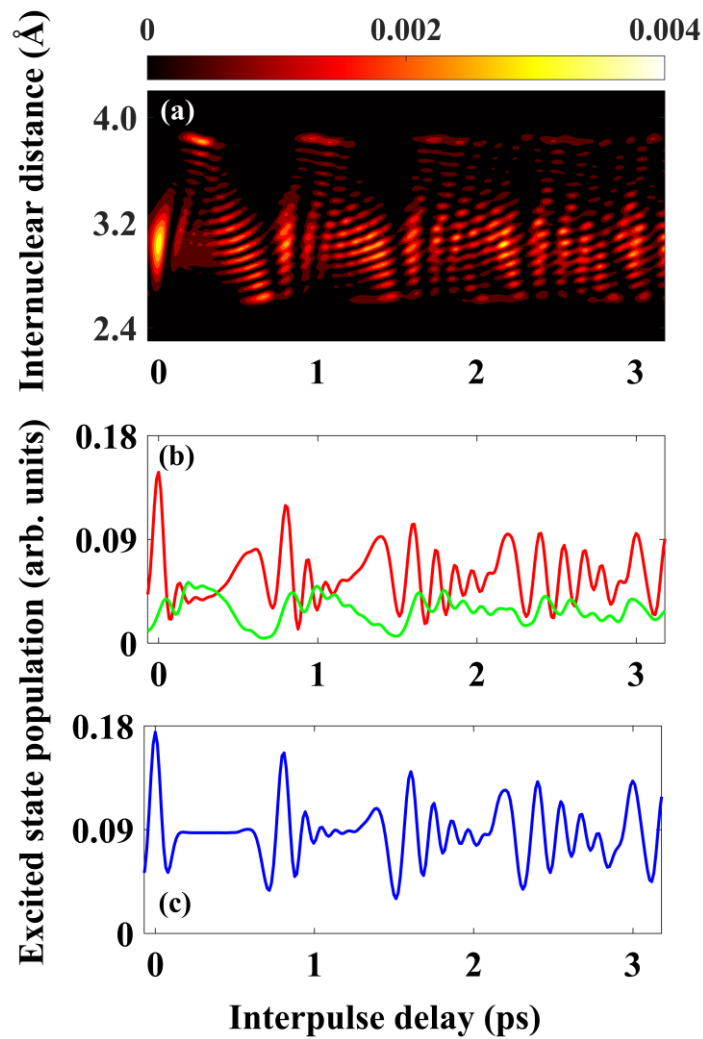


**Figure S3:** (a) Spatial mapping of excited state population as a function of interpulse delay after introducing a chirp of  $-2000 \text{ fs}^2$ . (b) Excited state population within the left well (shown in red) and the right well (shown in green) as a function of interpulse delay. (c) Total excited state population obtained by summing up both the contributions from the left and the right wells as a function of interpulse delay.

## Supplementary Information

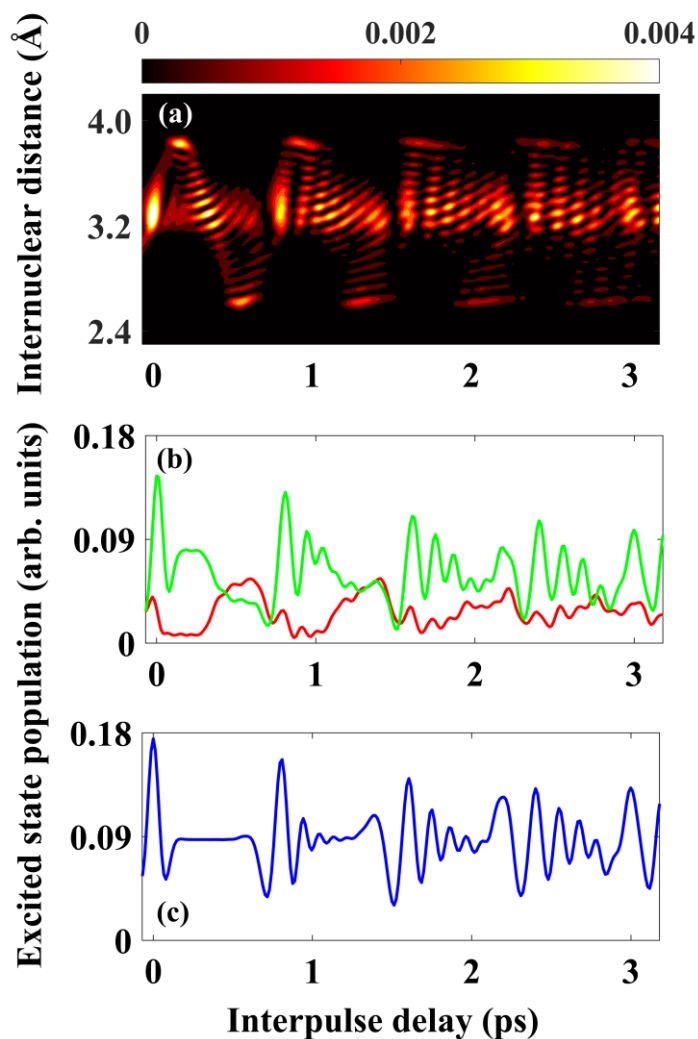


**Figure S4:** (a) Spatial mapping of excited state population as a function of interpulse delay after introducing a chirp of  $+1000 \text{ fs}^2$ . (b) Excited state population within the left well (shown in red) and the right well (shown in green) as a function of interpulse delay. (c) Total excited state population obtained by summing up both the contributions from the left and the right wells as a function of interpulse delay.

## Supplementary Information

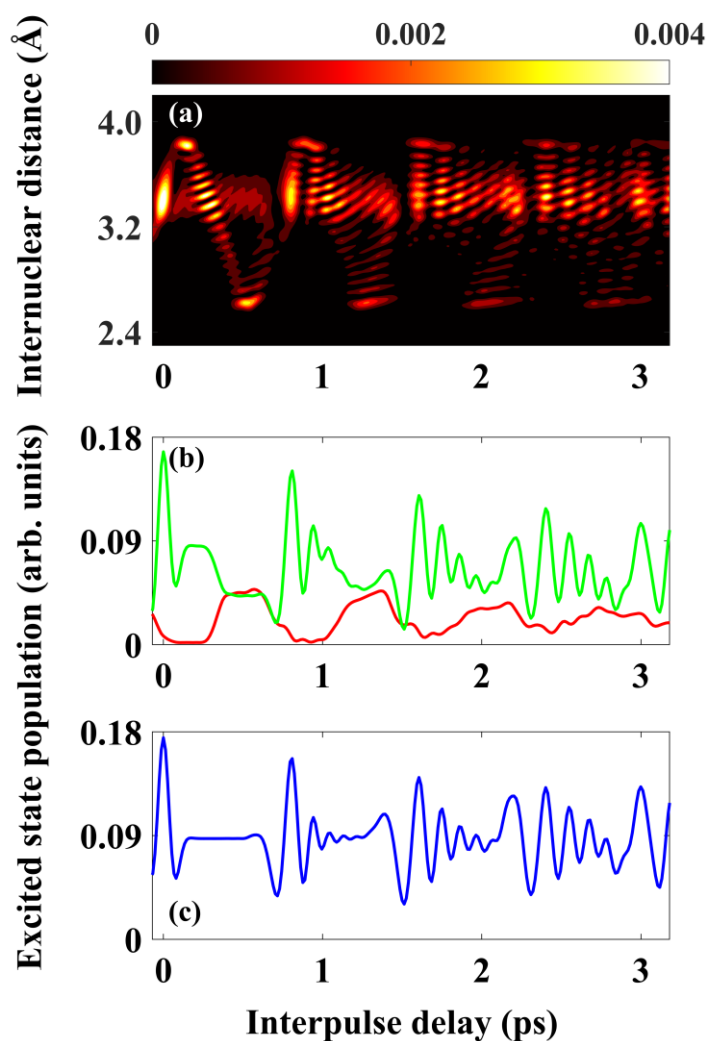


**Figure S5.** (a) Spatial mapping of excited state population as a function of interpulse delay after introducing a chirp of  $+2000 \text{ fs}^2$ . (b) Excited state population within the left well (shown in red) and the right well (shown in green) as a function of interpulse delay. (c) Total excited state population obtained by summing up both the contributions from the left and the right wells as a function of interpulse delay.

## Supplementary Information

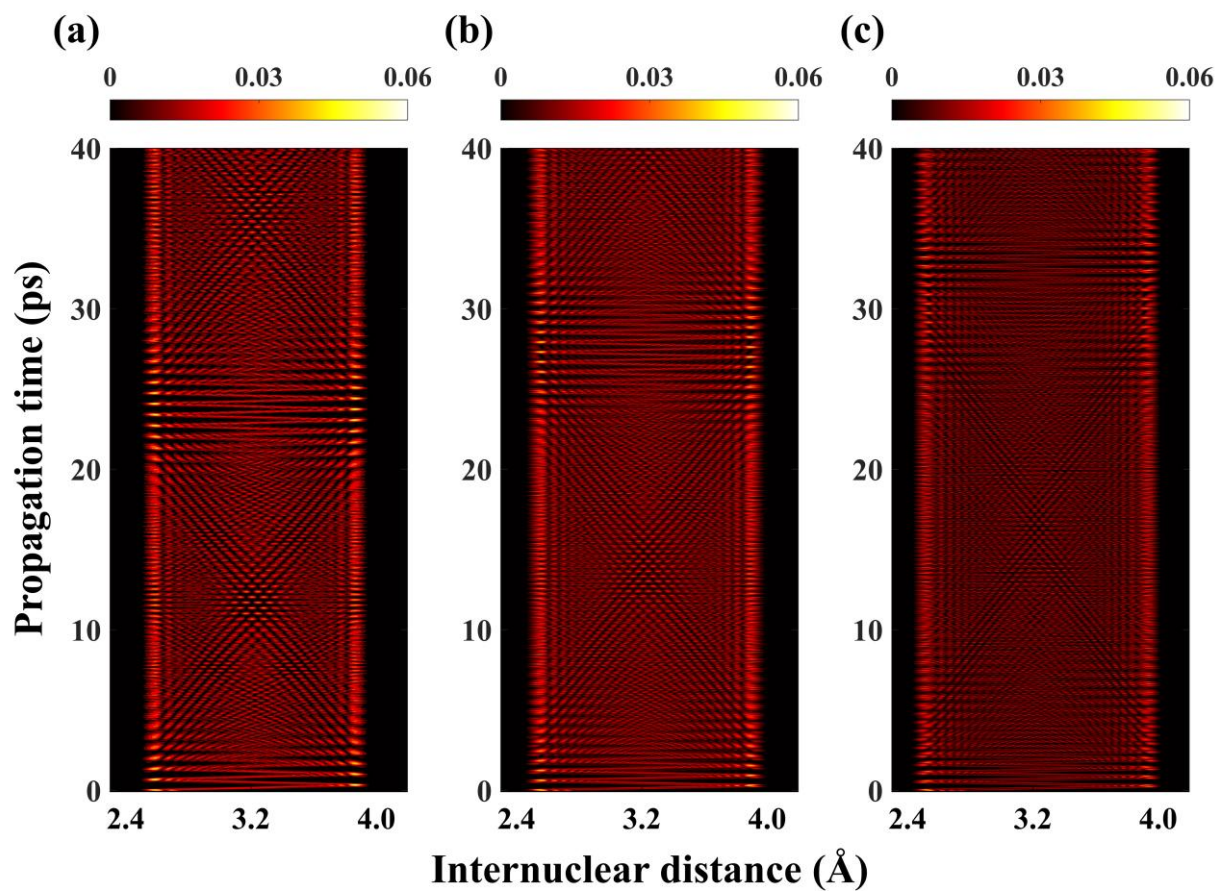


**Figure S6:** Simulated quantum carpet structure prepared by  $16,300\text{ cm}^{-1}$  excitation for  $E_b = 200\text{ cm}^{-1}$  for (a)  $\nu'' = 1$  (b)  $\nu'' = 2$ , (c)  $\nu'' = 3$ . The color bar corresponds to the absolute value of the complex WP in space and time and the unit of the color bar is  $\text{\AA}^{-1}$ .

## Supplementary Information

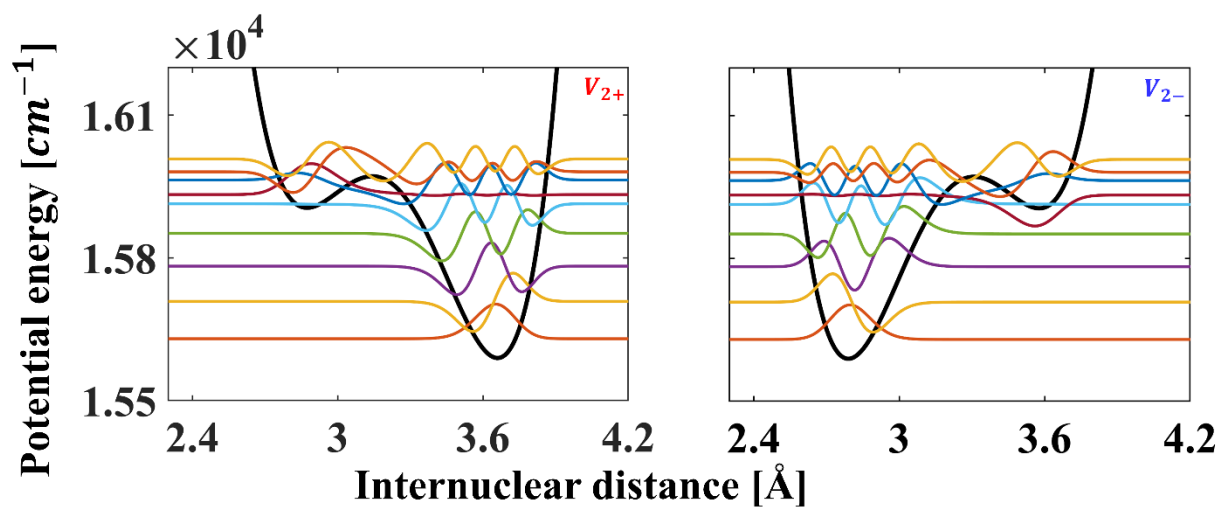


Figure S7: Wavefunctions for the asymmetric double well potentials.